samples of "pure" noble metals.[2,3] Typical results are shown in Figs. I, 4 and II, 3–7 of reference 1.

A theoretical account can be given if we assume that it is possible to construct wave packets, formed from distorted Bloch waves with energy near the surface of the Fermi-sea only, which correspond to a state of one electron localized in a volume equal to the volume per Mn ion, and which, for low concentration c, do not contribute to the conductivity.

The interaction between a Mn^{++} ion, which is in a ^6S state, and such an electron will remove the spin-degeneracy. The magnetic dipole interaction would give the energies $\pm E_1 = \pm(8\pi/3)5\mu^2|\chi(0)|^2$ with respect to the Fermi level, $\chi(r)$ being the orbital part of the wave function of these packets. The exchange interaction is of opposite sign and probably larger. Such a splitting may very well be of the order of a few °K. As a result of overlap and finite lifetime these local states will form a band of width ΔE. Both ΔE and E_1 will increase with increasing c.

The conduction electrons with energy in the intervals $\pm[E_1\pm\Delta E/2]$ give, due to resonance scattering, a negligible contribution to the current in an applied field. Therefore the conductivity is:

$$\sigma = \sigma_0[1+(\partial f_0/\partial E_1)\Delta E], \tag{1}$$

where f_0 is the Fermi function without field and σ_0 is the conductivity in the absence of this resonance effect. Equation (1) can reproduce the $R-T$ curves for low c between $T=0$ and the minimum very well. Some experimental values of E_1 and ΔE as a function of c are shown in Fig. 1.

There will be, apart from resonance scattering and coulomb scattering, another process which we will call nonresonance scattering. This occurs for all electrons and consists of a second order transition with a "local" state as a virtual intermediate state. We calculated it as if all conduction electrons were at the Fermi level.

The contribution of the nonresonance scattering and the coulomb scattering to the total resistance will be of the same order of magnitude. If ψ_k is a Bloch wave normalized in the volume per Mn ion, the first is proportional to $|\int\psi_k^* V\chi d\tau|^4/E_1^2 = V_{k\epsilon}^4/E_1^2$, the latter to $|\psi_k^* U\psi_{k'}d\tau|^2$, where V is the effective field acting on the electron in the local state, and U is the effective perturbation in the lattice potential.

Calculating separately the contribution from Mn ions with one or both local states unoccupied, gives Eq. (2) with $H=0$.

In a magnetic field H the magnetic ions will be quantized according to $\cos\vartheta_m = m/j$, $m=-j, \cdots, j$ and distributed according to a Boltzmann law $\exp(-2m\mu H/kT)$. Moreover, the field will cause a perturbation of the local states:

$$E_m = \pm\lambda_m = \pm[\mu^2H^2+E_1^2+2\mu HE_1m/j]^{\frac{1}{2}}.$$

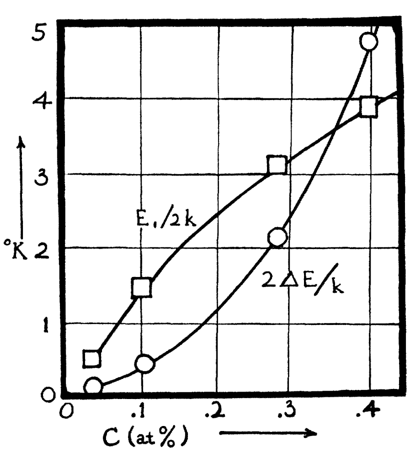

FIG. 1. Values of E_1 and ΔE as a function of c deduced from the experiments with the use of formula (1).

A calculation of the spin part of the perturbed wave functions and of the transition probabilities for ξ and η electrons separately leads to:

$$\begin{aligned} -(\partial f_{\xi(\eta)}/\partial t)_{n.r.} &= (f_{\xi(\eta)}-f_0)/\tau_{\xi(\eta)}, \\ 1/\tau_{\xi(\eta)} &= [N(\zeta_0)/4\pi^2\hbar]V_{k\epsilon}^4(P\pm Q); \\ P = \Sigma_m(x^{2m}/\lambda_m^2)[1&-f_0(-\lambda_m)f_0(\lambda_m) \\ &-\tfrac{1}{2}\{f_0(-\lambda_m)-f_0(\lambda_m)\}\{f_0(-2\lambda_m)-f_0(2\lambda_m)\}]/\Sigma x^{2m}, \\ Q = \Sigma_m(x^{2m}/2\lambda_m^3)&(\mu H+E_1m/j)\{f_0(-\lambda_m)-f_0(\lambda_m)\} \\ &\times\{2-f_0(-2\lambda_m)-f_0(2\lambda_m)\}/\Sigma x^{2m}. \end{aligned} \tag{2}$$

$N(\zeta_0)$ is the density of states at the Fermi level, $x=\exp(-\mu H/kT)$. For $H=0$, $Q=0$, $x=1$, and $\lambda_m=E_1$.

From (2) we find:

$$\begin{aligned} \sigma(H,T) &= \tfrac{1}{2}(\sigma_\xi+\sigma_\eta)[1+\tfrac{1}{2}BH^2(\sigma_\xi^2+\sigma_\eta^2)]^{-1}, \\ \sigma_{\xi(\eta)} &= (N_{\text{eff}}e^2/m_0)[1/\tau_{\xi(\eta)}+1/\tau_C+1/\tau_T]^{-1}. \end{aligned} \tag{3}$$

τ_C and τ_T are the effective collision times for coulomb and temperature scattering ($\tau_\xi\approx\tau_C\ll\tau_T$ at low temperatures). B is the coefficient determining the magnetoresistance of pure silver.

At low H we find $\Delta R/R\approx a(T,c)H^2$, with $a<0$ for low T and not too small c. At larger fieldstrength the $\Delta R/R$ *vs* H curves show saturation. The sudden increase of $\Delta R/R$ at low H for "large" c (see Fig. II, 5 of reference 1, $c=0.61$ atomic percent) will be due to the conductivity of the local states. It can be shown that this becomes important for this magnitude of c; in a magnetic field the energy of the local states differs at different Mn ions, the electrons can no longer make transitions from one ion to another, and the corresponding term in the conductivity will decrease rapidly in a magnetic field.

A further consequence of this model is an anomalous specific heat:

$$\rho c_V = \tfrac{2}{3}\pi^2k^2TN(\zeta_0) - nE_1(d/dT)\tanh(E_1/2kT),$$

where n is the number of Mn ions per unit volume. The local states could also lead to exchange interaction between the Mn ions; some of the irreproducible effects in the magnetoresistance, and the behavior of the susceptibility[4] seem to point to this direction.

A detailed account will be published in *Physica*.

[1] A. N. Gerritsen and J. O. Linde, Physica 17, 573, 584 (1951).
[2] E. Mendoza and J. G. Thomas, Phil. Mag. (7) 42, 291 (1951), where further literature may be found.
[3] D. K. C. MacDonald, Phil. Mag. (7) 42, 756 (1951).
[4] *Le Magnétisme* (Institut International de Coopération Intellectuelle, Paris, 1940), Vol. III, pp. 306 ff.

Multiple Scattering of Electrons in Nuclear Emulsions*

DALE R. CORSON
Cornell University, Ithaca, New York

(Received September 10, 1951)

THE Fowler[1] method for deducing the momentum of a fast particle from its multiple coulomb scattering is highly useful in nuclear emulsion work and several preliminary calibration measurements have been reported.[2–4] Recently extensive calibration measurements have been reported,[5–8] among them an abstract[5] of the results recorded here.

The results are best presented in terms of multiple scattering theory, the Snyder and Scott[9] version being chosen as the most convenient here. Snyder and Scott give normalized distribution curves for the probability $W(\eta, z)$ that the particle will be scattered through an angle η (projected on a plane) in traveling a distance z. η is measured in terms of a unit angle η_0, which is a function of the atomic number of the scattering material and of the mass and energy of the particle. z is measured in terms of the mean free path for scattering λ which is a function of the atomic number of both the scatterer and the particle and of the particle's energy. Using Snyder and Scott's prescription for calculating these quantities, we find for singly-charged particles in Ilford G-5 emulsion that $\eta_0=1.39\ (m/\mu)(E^2-1)^{-\frac{1}{2}}$ degrees and $\lambda=0.160\ (E^2-1)/E^2$ mi-

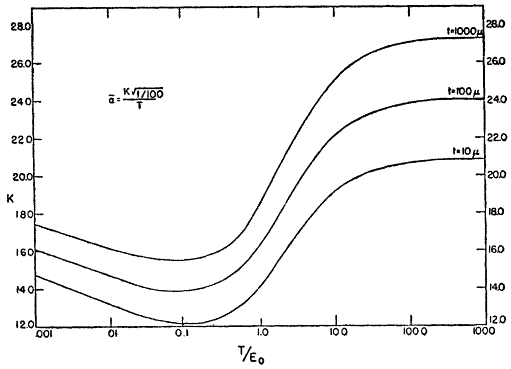

FIG. 1. The variation of the scattering constant K as a function of the ratio of kinetic energy to rest energy (T/E_0) for various cell lengths t.

crons where m and μ are masses of electron and scattered particle, respectively, and E is the ratio of the particle's kinetic energy to its total energy. To calculate mean scattering angles we must evaluate $\langle\eta\rangle_{Av}=\int\eta W(\eta)d\eta$. This must be done numerically, but Snyder and Scott give interpolation data which make the calculation particularly simple. We can write

$$\langle\eta\rangle_{Av}=z^{\frac{1}{2}}\int(\eta/z^{\frac{1}{2}})W(\eta)z^{\frac{1}{2}}(d\eta/z^{\frac{1}{2}})=z^{\frac{1}{2}}\int Rf(R)dR=z^{\frac{1}{2}}\langle R\rangle_{Av},$$

where $R=\eta/z^{\frac{1}{2}}$ and $f(R)=z^{\frac{1}{2}}W(\eta)$. We get $f(R)$ *vs* R for various z's directly from Snyder and Scott's data. $\langle R\rangle_{Av}$ increases from about 1.5 to 1.8 as z varies from 100 to 3000, so that $\langle\eta\rangle_{Av}$ increases somewhat more rapidly than $z^{\frac{1}{2}}$. $\langle R\rangle_{Av}$ is calculated using only values of R out to $4\langle R\rangle_{Av}$ and in the measurements all angles greater than four times the final mean are disregarded. With $\langle\eta\rangle_{Av}$ evaluated, we get mean angle in degrees from $\langle\theta\rangle_{Av}=\langle\eta\rangle_{Av}\eta_0$. This gives the mean projected angle between successive tangents to points on the track separated by a distance $x=z\lambda$. In the Fowler method we measure the mean angle $\langle\alpha\rangle_{Av}$ between successive chords. If the distribution of angles were gaussian the relationship would be $\langle\alpha\rangle_{Av}=(2/3)^{\frac{1}{2}}\langle\theta\rangle_{Av}$, and this is what is used in this discussion. The distribution is not quite gaussian, but out to angles of four times the mean, small error is introduced by this assumption. We have finally that

$$\langle\alpha\rangle_{Av}=(2/3)^{\frac{1}{2}}(x/\lambda)^{\frac{1}{2}}\langle R\rangle_{Av}\eta_0.$$

It is convenient to calculate $\langle\alpha\rangle_{Av}$ in terms of the particle's kinetic energy (T) and of the ratio (T/E_0) of its kinetic energy to its rest energy. When we do this, using the values of η_0 and λ appropriate to the G-5 emulsion we get

$$\langle\alpha\rangle_{Av}=1.46x^{\frac{1}{2}}\langle R\rangle_{Av}(1+T/E_0)/[T(2+T/E_0)],$$

where α is measured in degrees, x in microns, and T and E_0 in Mev. $\langle R\rangle_{Av}$ is a function of x/λ and therefore is a function of x and T/E_0, so that we can then write $\langle\alpha\rangle_{Av}=k(x, T/E_0)x^{\frac{1}{2}}/T=K(x, T/E_0)(x/100)^{\frac{1}{2}}/T$ where $K=10k$, since it is customary to refer all measurements to cell lengths of 100 microns. K *vs* T/E_0 for various x's is plotted in Fig. 1.

Measurements have been made on approximately 90 cm of electron and positron track produced by particles of well defined energy. The particles were produced in a thin radiator by synchrotron radiation and passed through $\frac{1}{16}$ in. of aluminum and about $\frac{1}{2}$ in. of air before striking the emulsion. Only the first 1000 microns of tracks which entered the emulsion at the air surface were used for measurement. The tracks were nearly parallel with the long edge of the plate (x-axis). The y-coordinate was read to 0.1μ (using an eyepiece scale for which the smallest division corresponded to 0.93μ) at intervals of 100μ. X-axis travel was produced by a micrometer screw drive on the microscope stage.

TABLE I.

Particle	Cm of track	$K(100)$
40 Mev positrons	13.4	24.6 ± 1.0
113 Mev positrons	29.3	23.0 ± 0.7
196 Mev positrons	21.9	25.0 ± 0.8
196 Mev electrons	20.8	27.3 ± 0.8
283 Mev positrons	6.5	25.0 ± 1.5

The "noise" in the measurements has been eliminated by using a method similar to one previously outlined.[3] Examination of the curves in Fig. 1 shows that for cell lengths between 10 and 1000 mμ and for T/E_0's from 0.1 to 1000 the variation of the scattering constant with cell length can be well represented by $\langle\alpha(x)\rangle_{Av}=K(100, T/E_0)(X/100)^{0.56}T^{-1}=\langle\alpha(100)\rangle_{Av}(X/100)^{0.56}$. We can show that the second differences measured in the Fowler scheme are given by $\langle D_m(x)\rangle_{Av}^2=\langle\alpha_t(100)\rangle_{Av}^2X^{3.12}/100^{1.12}+6\langle\Delta y\rangle_{Av}^2$ where m is used to indicate measured values and t true values. $\langle\Delta y\rangle_{Av}$ is the mean uncertainty of the y coordinate readings. Thus a plot of $\langle D_m(x)\rangle_{Av}^2$ *vs* $X^{3.12}$ yields $\langle\alpha_t(100)\rangle_{Av}$ and thus $K(100, T/E_0)$. For large T/E_0 this is the number commonly referred to as the scattering constant.

The results of the measurements, using this noise elimination method, are shown in Table I. A weighted average of all the individual measurements gives a $K(100)=25.1\pm0.6$. (The use of the $X^{0.56}$ variation in the noise elimination gives a K somewhat lower than the one reported in the abstract.)

I am indebted to Mrs. Margaret R. Keck for most of the observations on which these measurements are based.

* This work was supported by the ONR.

1 P. H. Fowler, Phil. Mag. **41**, 169 (1950).
2 U. Camerini *et al.*, Phil. Mag. **41**, 701 (1950).
3 D. R. Corson, Phys. Rev. **80**, 303 (1950).
4 L. Voyvodic and E. Pickup, Phys. Rev. **81**, 471 (1951); **81**, 890 (1951).
5 D. R. Corson, Phys. Rev. **83**, 217 (1951).
6 K. Gottstein *et al.*, Phil. Mag. **42**, 708 (1951).
7 L. Voyvodic and E. Pickup, Phys. Rev. (to be published).
8 Berger, Lord, and Schein, Phys. Rev. **83**, 850 (1951).
9 H. S. Snyder and W. T. Scott, Phys. Rev. **76**, 220 (1949).

Discharge Mechanism in Argon Counters

LAURA COLLI, UGO FACCHINI, AND EMILIO GATTI
C.I.S.E.—Piazza Cimitero Monumentale, Milano, Italy
(Received September 10, 1951)

A PREVIOUS paper[1] reported a study on the behavior of argon counters in proportional and Geiger regions.

By observing the shapes of the pulses obtained from α and β particles in the counter, it has been found that, in these regions, the mechanisms responsible for the discharge building-up are the photoelectric effect on the cathode and, as is known, the α-Townsend process on the wire.

The argon employed in the afore-mentioned experiments was 98 percent pure, purified on hot calcium later.

We endeavored to establish the validity of our observations, as dependent upon the purity of argon, in a later series of experiments.

The argon to be employed was analyzed by measurement of drift velocity of electrons, using an ionization chamber containing a beam of collimated α-particles.[2] These observations showed that the argon circulated on hot calcium was about 99.7 percent pure, containing carbon dioxide as the impurity most expected.

In order to prove the validity of these results, argon of purity better than 99.9 percent from different origins (spectral argon Lindemann, soldering argon, and commercial argon circulated on calcium magnesium alloy at 450°C[2]) was used, mixed with about 0.1 percent of carbon dioxide. This mixture behaved in the counters like argon purified as in reference 1.

The 99.9 percent pure argon (without carbon dioxide), as studied in a preliminary way, showed that other processes are acting in the discharge, together with the photoelectric effect; these processes are due to metastable excited states of argon atoms produced in the avalanche.

As is known metastable atoms generally produce secondary electrons by impact on impurities contained in the gas or at the